Soft Matter

HYDROGEL COMPOSITE MIMICS BIOLOGICAL TISSUES

Journal:	*Soft Matter*
Manuscript ID	SM-ART-04-2022-000505.R1
Article Type:	Paper
Date Submitted by the Author:	19-May-2022
Complete List of Authors:	Horkay, Ferenc; National Institute of Child Health and Human Development, Section on Quantitative Imaging and Tissue Sciences Basser, Peter; National Institute of Child Health and Human Development

SCHOLARONE™
Manuscripts

HYDROGEL COMPOSITE MIMICS BIOLOGICAL TISSUES

Ferenc Horkay* and Peter J. Basser

Section on Quantitative Imaging and Tissue Sciences, *Eunice Kennedy Shriver* National Institute of Child Health and Human Development, National Institutes of Health, Bethesda, MD 20892, USA

ABSTRACT

A novel composite hydrogel was developed that shows remarkable similarities to load bearing biological tissues. The composite gel consisting of a poly(vinyl alcohol (PVA) matrix filled with poly(acrylic acid) (PAA) microgel particles exhibits osmotic and mechanical properties that are qualitatively different from regular gels. In the PVA/PAA system the swollen PAA particles "inflate" the PVA network. The swelling of the PAA is limited by the tensile stress P_{el} developing in the PVA matrix. P_{el} increases with increasing swelling degree, which is opposite to the decrease of the elastic pressure observed in regular gels. The maximum tensile stress P_{el}^{max} can be identified as a quantity that defines the load bearing ability of the composite gel. Systematic osmotic swelling pressure measurements have been made on PVA/PAA gels to determine the effects of PVA stiffness, PAA crosslink density, and Ca^{2+} ion concentration on P_{el}^{max}. It is found that P_{el}^{max} increases with the stiffness of the PVA matrix, and decreases with (i) increasing crosslink density of the PAA and (ii) increasing Ca^{2+} ion concentration. Small angle neutron scattering (SANS) measurements indicate only a weak interaction between the PVA and PAA gels. It is demonstrated that the osmotic swelling pressure of PVA/PAA composite gels reproduces the osmotic behavior of healthy and osteoarthritic cartilage.

Keywords: osmotic swelling pressure, composite gel, poly(vinyl alcohol), poly(acrylic acid), cartilage, small angle neutron scattering

Corresponding author: Ferenc Horkay, e-mail: horkayf@mail.nih.gov

2

INTRODUCTION

Recent studies have shown the potential of hydrogels to mimic the biomechanical properties of the extracellular matrix (ECM).[1-12] The ECM is a complex environment consisting of collagen, proteoglycans (PGs) and other soluble molecules, ions and water. In cartilage the bottlebrush-shaped aggrecan molecules self-assemble into large microgel-like aggregates composed of approximately 100 aggrecan molecules, which are noncovalently linked to a linear hyaluronic acid (HA) chain.[13-20] These large aggrecan-HA assemblies are enmeshed in a network of type II collagen fibers. PG assemblies swell against the confining collagen network producing an osmotically pre-stressed tissue matrix that is capable of resisting mechanical loads. Recent research revealed the role of large microgel-like aggrecan-HA aggregates in improving load bearing, dimensional stability and lubricating ability.[21-26] The remarkable insensitivity of the aggrecan-HA microgels to changes in the ionic environment, particularly to calcium ions is essential for normal cartilage and bone function.

Understanding the physical-chemical properties of microgels is important not only because PGs form microgels in the ECM but also because these materials have a great potential in biomedical and materials science applications. "Microgels" are polymeric gel "particles" composed of a network whose dimensions are often on the order of molecular or micron dimensions typical of colloidal particles, which are capable of swelling in a solvent dependent on the "solvent quality", and the extent of cross-linking in the network, with a higher crosslink density normally leading to reduced maximum extent of swelling. In many cases the swelling and stiffness of microgel particles can be tuned by external stimuli such as temperature, pH, ionic strength and electric field. Although the chemical composition and the equilibrium thermodynamic properties of microgels are similar to those of the corresponding macrogels, there are significant differences between the two forms of these chemically identical materials. For example macrogels exhibit viscoelastic behavior, while microgels are low viscosity dispersions. Furthermore, the response of macrogels to changes in the environment (e.g., temperature, ionic strength, pH) is relatively slow; in contrast, microgels response rapidly to such changes. This ability enables the use of microgels in different applications, such

3

as chemical and biological sensors, controlled release, drug delivery, etc.[27-33]

Engineered ECM is widely used for tissue engineering and regenerative medicine applications. Significant effort is being made to develop biomimetic hydrogels to facilitate cartilage tissue replacement, repair, and regeneration. Owing to their high water content (> 90%) hydrogels are usually viscoelastic materials and resemble the properties of articular cartilage. Various natural and synthetic polymers, such as HA, collagen, poly(vinyl alcohol) (PVA), have been used to replace diseased or damaged cartilage tissue.[34-44] From the materials science perspective, we view cartilage as a natural fiber-reinforced composite hydrogel consisting of mainly PGs (10-15%), type II collagen (10-20%), chondrocytes (cartilage cells, 1-5%) and approximately 65-80% water by weight. PVA exhibits excellent biocompatibility and is a particularly promising biomaterial in tissue engineering applications. PVA hydrogels mimic the water content of cartilage and possess low friction coefficient, which is a basic requirement for joint lubrication. Clinical studies have shown that PVA is a potential synthetic alternative to native cartilage replacement. Highly swollen PVA hydrogels have been successfully used for implants that reconstruct meniscus function and prevent the progression of osteoarthritis (OA) in cartilage.[46-49]

Hydrogels designed for orthopedic applications must possess comparable mechanical properties to the native tissue. Although certain properties of PVA gels resemble the behavior of cartilage tissue (e.g., stiffness, high water content), regular PVA gels are too week to resist the high compressive loads imposed on joint surfaces. Several attempts have been made to improve the mechanical strength of PVA hydrogels such as crosslinking of the polymer molecules (e.g., by dialdehydes), introducing filler particles (e.g., glass), inducing partial crystallization (e.g., by freeze thawing).[50-55] In recent years new preparation techniques have been developed (e.g., in situ co-precipitation, sol–gel method, solvent casting technology). The in-situ co-precipitation method has received particular attention because it shows similarity to the in situ mineralization of hydroxyapatite in bone.[56-58]

Knowledge of the role of various components and their interactions in defining the mechanical properties of ECM is essential for developing advanced tissue engineering/regenerative medicine strategies. Here we describe a novel composite

4

hydrogel that mimics the biomechanical properties of cartilage ECM. The composite gel consists of a PVA network filled with small (≈10 μm) poly(acrylic) acid (PAA) gel particles. The present composite gel is conceptually different from the traditional filler reinforced systems. Inorganic fillers (e.g., fumed silica) are solid particles that improve the mechanical properties (elastic modulus, etc.) of the gels by making additional contacts between the polymer chains. However, in the PVA/PAA gel the "filler" is a soft gel that inflates the surrounding matrix.

Despite the many obvious material differences between cartilage and PVA/PAA hydrogels, these systems share an important common feature, namely, that their networks are both in tension in the absence of external loading. In cartilage, intracellularly synthesized aggrecan bottlebrushes are secreted into the ECM, where they form supramolecular aggregates with HA stabilized by a link protein.[16-19] The collagen network is inflated by the highly swollen aggrecan/HA complexes enmeshed in the matrix. The osmotic swelling pressure of the charged PG assemblies keeps the collagen in a pre-stressed state. In PVA/PAA gels the PAA particles inflate the PVA matrix. We found that the PVA/PAA hydrogel exhibits qualitatively similar mechanical and osmotic properties to cartilage, which renders this system an appropriate biomimetic model of cartilage.[105] In this model the PVA network corresponds to the collagen matrix while the PAA microgel phase plays the role of the PG.

It has been recognized that pre-stress plays important role in the biomechanics of various biological tissues. However, the consequences of pre-stress and tissue inflation on the load bearing properties have not yet been previously explored. An elegant approach based on the tensegrity model was proposed to elucidate how mechanical stresses are transmitted to individual cells and transduced into a biochemical response.[59,60]

We argue that pre-stress is a key determinant of the unique mechanical properties of load bearing biological tissues, particularly those made of soft and "squishy" polymeric materials. Therefore, systematic studies made on inflated model hydrogels is expected to provide invaluable information on the effect of various factors (matrix stiffness, swelling pressure, charge density of the gel particles, etc.) on the macroscopic mechanical/swelling properties, and ultimately the load bearing ability of these systems.

5

Similar information cannot be obtained from measurements made on biological tissues because their composition and physical properties (e,g., stiffness, charge density) cannot currently be independently and systematically varied.

　　　This paper is organized as follows: First, we discuss the osmotic behavior of the two polymeric components (PVA and PAA gels) individually. The effect of gel stiffness on the osmotic swelling pressure and elastic pressure is determined by the osmotic stress technique. Then, we present results obtained for PVA/PAA composite hydrogels. We systematically vary (i) the stiffness of the PVA matrix, (ii) the crosslink density of the PAA gel particles, and (iii) the Ca^{2+} ion concentration of the equilibrium solution. Small angle neutron scattering (SANS) measurements are made to quantify the interactions between the two polymeric components over a broad range of length scales. A comparison is made between the osmotic response of PVA/PAA hydrogels and swelling pressure data reported for healthy and osteoarthritic cartilage in the literature.

THEORETICAL SECTION

Swelling and elastic properties of gels

　　　The Flory-Rehner model[61-63] assumes additivity of the free energy of mixing of the polymer and solvent molecules (ΔF_{mix}), and the free energy of elastic deformation of the network chains (ΔF_{el}),

$$\Delta F = \Delta F_{mix} + \Delta F_{el} \tag{1}$$

　　　The osmotic swelling pressure Π_{sw} is is the sum of two components: the osmotic mixing pressure Π_{mix} that tends to expand the gel and the elastic pressure Π_{el} that counteracts Π_{mix} and limits gel swelling. At equilibrium we have

$$\Pi_{sw} = - \partial \Delta F / \partial V = \Pi_{mix} + \Pi_{el} \tag{2}$$

where V is the volume of the gel.

　　　Non-zero values of Π_{sw} can be achieved by equilibrating the gel with a solution of

6

an osmotic stressing agent of known osmotic pressure[64,65] or vapor pressure[66-68], or by squeezing water out of the swollen network by applying an external mechanical (hydrostatic) pressure.[69,70]

In the semidilute concentration regime Π_{mix} can be satisfactorily described by the Flory-Huggins expression[71-76]

$$\Pi_{mix} = -(RT/V_1) [\ln(1-\varphi) + \varphi + \chi_0\varphi^2 + \chi_1\varphi^3] \tag{3}$$

where V_1 is the partial molar volume of the solvent, φ is the volume fraction of the polymer, χ_0 and χ_1 are interaction parameters related to the second and third virial coefficients, R is the universal gas constant and T is the absolute temperature.

To estimate the elastic free energy of polymer networks several models have been proposed. In the classical models of Wall and Flory, and James and Guth the polymer chains are idealized, volumeless, Gaussian chains.[77-82] More advanced models take into account inter-chain or 'entanglement' interactions defined in terms of topological constraints due to chain uncrossability and correlations arising from molecular packing of the network chains. For our purposes, a minimal statistical mechanical model of rubber elasticity must incorporate three main features: (i) connected network of flexible polymer chains, (ii) entanglement constraints, and (iii) finite volume of the network chains. The Localization Model (LM) directly addresses the interchain interactions, which can be large in the condensed state, just as molecules in a liquid state have larger intermolecular interactions than when in a gaseous state.[83-85,99] An examination of the LM in comparison stress-strain data reported in the literature indicated that this elegantly simple and conceptually clear model of rubber elasticity provided a good description of the experimental results both in the swollen and dry states.[86]

In the LM the elastic free energy of the polymer network consisting of flexible chains is given as

$$\Delta F_{LM} = (G_c/2) [(\lambda_x^2 + \lambda_y^2 + \lambda_z^2 - 3)/3] + G_e [(\lambda_x + \lambda_y + \lambda_z - 3)/3 \tag{4}$$

where λ_x, λ_y and λ_z are deformation ratios along the x, y and z directions. The shear

modulus G_c is proportional to the number of elastic chains ν in the network

$$G_c = C_0 \, \nu \, k_B \, T \tag{5}$$

where k_B is the Boltzmann constant. C_0 depends on the details of the network structure (dangling ends, junction functionality, etc.). In the model of Wall and Flory $C_0 = 1$, while in the model of James and Guth, $C_0 = 1/2$. The entanglement contribution G_e to the network free energy contains a cross-term proportional to G_c,

$$G_e = \gamma \, G_c + G^*_N \tag{6}$$

In equation 6, the γ parameter is an empirical parameter describing the cross-correlation of the crosslinking on the inter-chain entanglement interaction. The crosslink independent contribution (G^*_N) to G_e is identified with the independently measurable plateau modulus of the polymer melt, G^*_N.[83,84] The localization model can be extended to swollen networks by introducing a swelling factor λ_S.[99] In the case of isotropic swelling $\lambda_S = \lambda_X = \lambda_y = \lambda_z = (V/V_d)^{1/3}$, where V and V_d are the volumes of the swollen and dry networks, respectively.

In many network systems encountered in biological materials, the chains are relatively stiff so that the elasticity model based on a flexible chain model no longer applies. In the limit of small enough deformations, however, where linear elasticity still applies, we may still treat such materials as being Hookean so that the standard rubber elasticity model can be formally derived even from a continuum perspective, but we cannot expect this model to be predictive over a large range of deformations.

Vilgis and Edwards adopted an idealized model of such semi-flexible polymer networks as a collection of rods connected by freely-jointed tethers where it was found that the change of free energy of the network arising from altering the network junction points rather than deforming chains gave to a strongly non-linear change in the network free energy $\Delta F(\text{Vilgis-Edwards})$ of the form, $\Delta F(\text{Vilgis-Edwards}) \sim \exp\left[(\lambda_x^2 + \lambda_y^2 + \lambda_z^2)\right]$, at large network deformations.[87] Lin et al.[98] introduced a model that interpolated the exact low deformation scaling relation for ΔF for deformation in the linear elasticity

8

regime and at the same recovered the asymptotic scaling form for ΔF for large deformations derived by Vilgis and Edwards for the semi-flexible polymer network. (The rather complex integral equation-based theory of Edwards and Vilgis only allowed for limiting asymptotic behavior of the network.). We emphasize again that the entropic elasticity in this rod network model derives entirely from the deformation of the *junction positions* rather than from stretching the network polymer chains, so the physics is quite different from the flexible chain network model. The specific expression for the elasticity of semi-flexible polymer networks deduced from the arguments of Lin et al.[98] provides a simple closed form relation for ΔF(semi-flexible) that can be expected to apply to many networks involving stiff polymers,

$$\Delta F(\text{semi-flexible}) = (G_c /2b) \left\{ \exp\left[b \left[(\lambda_x^2 + \lambda_y^2 + \lambda_z^2 - 3) \right]/ 3 - 1 \right] - 1 \right\} \qquad (7)$$

where G_c scales with the number of cross-links as in chain elasticity of flexible polymer networks and *b* is a parameter that characterizes the amount of deformation required before non-linear effects of deformation of the network junctions makes a prevalent contribution to the network elasticity. Interestingly, it was then realized after deriving eq. (7) that this functional form is of the same general form as the purely phenomenological "Fung hyperelasticity model" that has been employed in many studies of the elasticity of many biological materials.[88,100-102] This lends some credence to the model in the applications considered in the present paper. Lin et al.[98] also extended this semi-flexible chain model to address interchain interactions.

Small angle neutron scattering

Small-angle scattering provides information on the structure and interactions within polymer solutions and gels over a broad range of length scales. In a polymer solution of overlapping polymer chains, the scattering intensity arising from thermodynamic concentration-fluctuations is given by the Ornstein-Zernike expression for the structure factor[88.89]

9

$$I_{SOL}(q) = a \frac{kT(\rho_P - \rho_S)^2 \varphi^2}{K_{OS}} \frac{1}{1+(q\xi)^2}$$

(8)

where ρ_p and ρ_s are the scattering length densities of the polymer and solvent, respectively, K_{OS} [$= \varphi(\partial\Pi_{mix}/\partial\varphi)$] is the osmotic compression modulus of the solution, ξ is the polymer-polymer correlation length, a is a constant and kT is the Boltzmann factor. In equation 8, q is the scattering wave vector, i.e., $q = (4\pi/\lambda)\sin(\theta/2)$, where λ and θ are the wavelength of the incident radiation and the scattering angle, respectively.

Gels generally contain static inhomogeneities frozen in by the crosslinks, which contribute to the scattering response $I_{ST}(q)$.[90=93]

The total scattering intensity from a polymer gel is taken to be the sum of dynamic (solution-like) and static contributions,

$$I_{GEL}(q) = I_{DYN}(q) + I_{ST}(q)$$

(9)

where the functional form of the first term is similar to that of the corresponding polymer solution while the second term depends on the particular network system.

In many neutral gels the scattering form structural inhomogeneities can be described by a Debye-Bueche structure factor and $I_{GEL}(q)$ is given by

$$I_{GEL}(q) = I_{DYN}(q) + \frac{I_{ST}(0)}{(1+q^2\Xi^2)^2}$$

(10)

where $I_{ST}(0)$ is the extrapolated intensity at $q = 0$ and Ξ is the characteristic size of the inhomogeneities in the network.[94]

In gels comprised of polyelectrolyte chains the static component displays a power law behavior,

$$I_{ST}(q) = A\ q^{-m}$$

(11)

where m is a constant.[73-76] Such a power-law scattering intensity is indicative of fractal-

10

like structures. For scattering from three-dimensional objects with fractal surface, the power law exponent is negative - $(6 - D_s)$, where D_s is the fractal dimension of the surface $(2 < D_s < 3)$. $D_s = 2$ represents a smooth surface.

MATERIALS AND METHODS

Gel preparation

Poly(vinyl-alcohol) (PVA) gels were made by crosslinking with glutaraldehyde at pH = 1.0 in aqueous solutions.[93] For the experiments a fully hydrolyzed and fractionated PVA sample was used ($M_{w,PVA}$ = 110 kDa). Crosslinks were introduced at 4% (w/w) polymer concentrations, the molar ratio of monomer units to the molecules of crosslinker was 200. Gels were cast between two glass microscope slides with 2 mm thick spacers. After gelation the samples were equilibrated with 100 mM NaCl solution to remove HCl and uncrosslinked polymer (sol fraction). Then the gels were dried in an oven at 95 °C, reswollen in 100 mM NaCl solution for 24 hours, and exposed to two (PVA1), four (PVA2) six (PVA3) and eight (PVA4) cycles of freezing for 12-14 hours at $-$ 20 °C and thawing the samples for 10 hours at 25 °C.

The preparation of polyacrylic acid (PAA) gels has been described previously.[71,72] Poly(acrylic acid) gels were synthesized by free-radical copolymerization of partially neutralized acrylic acid and *N,N'*-methylenebis(acrylamide) in aqueous solution. The monomer concentration was 30% (w/w). The concentration of the crosslinker was 0.3 (PAA1), 0.6 (PAA2), 0.9 (PAA3) and 1.2 % (PAA4). In the initial mixture 35% of the monomers were neutralized by sodium hydroxide. After the components were mixed, dissolved oxygen that would inhibit the polymerization reaction was eliminated by bubbling nitrogen through the solution. The polymerization reaction was initiated by ammonium persulfate (0.5 g/L). After gelation the acrylic acid units were first neutralized with NaOH solution and then dried at 90 °C for 48 hours. The dry polymer was ground into a powder having an average particle size less than 10 microns.

PVA/PAA composite gels were prepared by crosslinking PVA in solution containing PAA particles. In the initial solution the concentrations of both polymers were 4%. First the HCl was added to the solution (pH ≈ 1) to suppress the swelling of

11

PAA. Then the crosslinker glutaraldehyde was added to the suspension. The molar ratio of the monomer units to the crosslinker was the same as in the pure PVA gels. The composite gels were treated by the freeze thaw process similarly to the PVA gels. The sample code is defined by the composition and the code of the corresponding PVA and PAA gel. For example, PVA1/PAA1 is a composite gel made by crosslinking a PVA solution containing PAA particles (crosslinker concentration: 0.3 %) and applying 2 freeze-thaw cycles.

Osmotic stress measurements

Gels were equilibrated with poly(vinyl pyrrolidone) (PVP) solutions (molecular weight: 29 kDa) of known osmotic pressure.[64,65,95] A semi-permeable membrane was used to prevent penetration of the PVP into the network. When equilibrium was reached, the polymer concentration in both phases was measured. This procedure yields for each gel the dependence of the osmotic swelling pressure on the polymer concentration.

SANS measurements

SANS measurements were made on the NG3 instrument at NIST, Gaithersburg MD. The incident wavelength was 8 Å. The sample-detector distances were 1.2, 4 and 13.1 m corresponding to a wave vector range 0.005 Å^{-1} < q < 0.1 Å^{-1}. The ambient temperature during the experiments was 25 ± 0.1 °C. Gel samples were prepared in D_2O solutions in 2 mm thick sample cells. After azimuthal averaging, corrections for incoherent background, detector response and cell window scattering were applied.[96]

RESULTS AND DISCUSSION

Osmotic and elastic properties

PVA and PAA gels

Figure 1a shows the variation of the osmotic swelling pressure Π_{sw} as a function of the swelling degree 1/φ for four PVA gels. Network stiffness varies according to the series, PVA1 < PVA2 < PVA3 < PVA4. We see that Π_{sw} decreases with increasing gel

stiffness and with increasing swelling degree. At equilibrium with the pure diluent (100 mM NaCl solution) $\Pi_{sw} = 0$. The dashed red curve represents the osmotic mixing pressure for the crosslinked PVA calculated by equation 3 with $\chi_0 = 0.494$ and $\chi_1 = 0.$[97] The difference between Π_{mix} and Π_{sw} is the elastic pressure of the crosslinked polymer Π_{el} defined by eq. 2. At equilibrium with the pure solvent, $\Pi_{el} = \Pi_{mix}$. The inset shows that Π_{el} strongly increases with decreasing swelling ratio. The observed increase can be attributed to crystallization, and hydrogen bonding between the hydroxyl groups on the PVA chains. It is well documented in the literature that the freeze-thaw procedure promotes the crystallization of PVA.[51-54] Microcrystallites and other molecular associations can act as physical crosslinks.
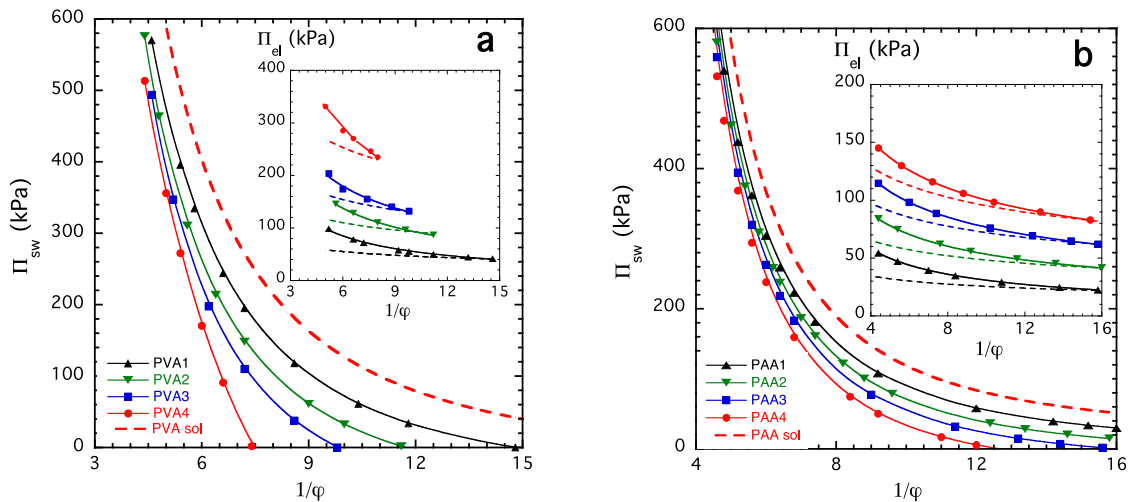
Figure 1. Π_{sw} vs $1/\varphi$ plots for PVA (figure a) and PAA (figure b) gels. Continuous curves through the data points are guides to the eyes. The red dashed curves show Π_{mix} vs $1/\varphi$ for the solutions of the corresponding uncrosslinked polymers. Inset: Π_{el} vs $1/\varphi$ plots. Dashed lines: prediction of the phantom network model (eq. 12); continuous curves: fits of eq. 13.

For isotropically swollen networks $[\lambda_x = \lambda_y = \lambda_z = (V/V_d)^{1/3}]$ the phantom network model and the Flory-Rehner theory indicates,

$$\Pi_{el} = \partial\{(3G_c/2)[(V/V_d)^{2/3} - 1]\}/\partial V = K\varphi^{1/3} \qquad (12)$$

13

where K is a constant (= $C_0 v^*$ RT, and v^* is the concentration of the elastic chains in the dry network).

The dashed curves in the inset show the elastic pressure predicted by the phantom network model (equation 12). This model underestimates the experimental data over the entire concentration range explored in the present experiment.

The continuous lines through the data point are fits to eq. 13 derived from the Localization Model for highly crosslinked gels[98,99]

$$\Pi_{el} = K_1 \varphi^{1/3} + K_2 \varphi^{4/3} \tag{13}$$

where K_1 and K_2 are constants (listed in Table 1).

Table 1.

Fitting parameters for the Π_{el} vs φ plots

Sample	K_1 (kPa)	K_2 (kPa)
PVA1	314	1236
PVA2	201	737
PVA3	127	738
PVA4	61	566
PAA1	46	193
PAA2	93	194
PAA3	143	195
PAA4	194	192

In Figure 1b, are shown the Π_{sw} vs $1/\varphi$ plots for PAA gels. These gels exhibit qualitatively similar behavior to the PVA gels. Evidently, Π_{sw} decreases with increasing

14

crosslink density and for high degrees of swelling Π_{sw} exceeds the values found for PVA gels. The inset in Figure 1b shows that in PAA gels the increase of the elastic pressure Π_{el} (= Π_{sw} - Π_{mix}) with decreasing swelling degree is less steep than in PVA gels. The fit to equation 12 is reasonable over an extended range of swelling (dashed lines), and the upturn of the Π_{el} vs $1/\varphi$ curves occurs at high polymer concentrations. The continuous lines show the fits to eq. 13 derived from the Localization Model. The values of the fitting parameters K_1 and K_2 are listed in Table 1.

In principle, eq. 3 is applicable only for uncharged gels. For polyelectrolytes an ion-dependent term must also be included. However, previous experimental studies, as well as molecular dynamics simulations indicated that the Flory–Huggins formalism is satisfactory for describing polyelectrolyte solution behavior in the presence of added salt having a concentration of physiological relevance and for polymer concentrations high enough for mean field theory to apply.[38] Simulations showed that under equilibrium conditions cancellation (i.e., enthalpy-entropy compensation) arises between the electrostatic and the counter-ion excluded volume contributions to the osmotic pressure. It was demonstrated that eq. 3, which accounts for neither electrostatic nor counter-ion excluded-volume effects, still fits both experimental and simulated data for various polyelectrolyte solutions.[73-76] Therefore, we do not include an explicit ionic contribution in the free energy function. This is an adequate approximation for the total free energy of the present gel system; however, ions play an important role in defining the osmotic swelling pressure of the PAA gels.

PVA/PAA composite gels

The situation in the composite gel is illustrated schematically in Figure 2. The PAA particles swell more than the PVA matrix resulting in a pre-stress that is generated in the inflated matrix.

15
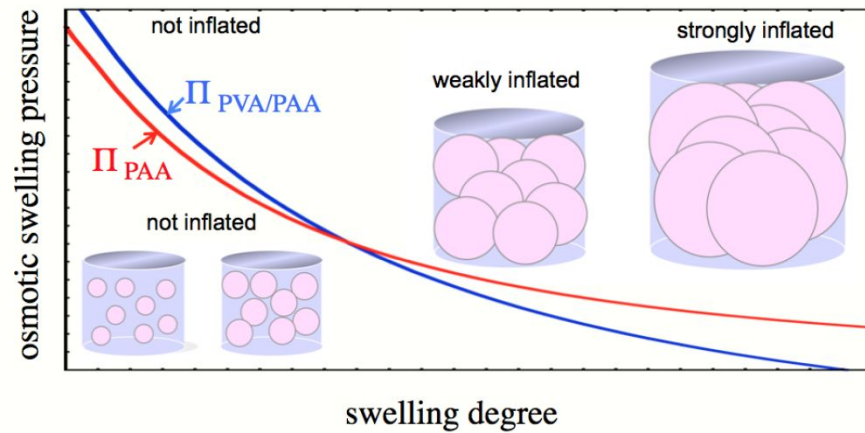
Figure 2. Schematic drawing illustrating gel inflation. Above the crossover point the enclosed gel particles swell more than the surrounding matrix. The matrix becomes inflated and prevents further swelling.

Figure 3 shows the variation of Π_{sw} as a function of $1/\varphi$ for PVA/PAA composite gels (ratio of PVA to PAA is 1:1). We focus on the effects of matrix stiffness (figure 3a), crosslink density of the PAA component (figure 3b), and Ca^{2+} ion concentration (figure 3c). Figure 3a shows that (i) the curves for the composite gels are always steeper than for the corresponding PVA gels (see Figure 1a) and (ii) displaced to lower swelling degrees. Decrease of the swelling degree is typical for gels containing filler particles. Physical interactions between the filler and the polymer matrix (e.g., adsorption) are expected to play a similar role as chemical crosslinks. Furthermore, the secondary structure of the filler (e.g., interparticle aggregates) may also affect gel stiffness. The dashed curve shows the variation of the swelling pressure of the PAA as a function of $1/\varphi$.

16
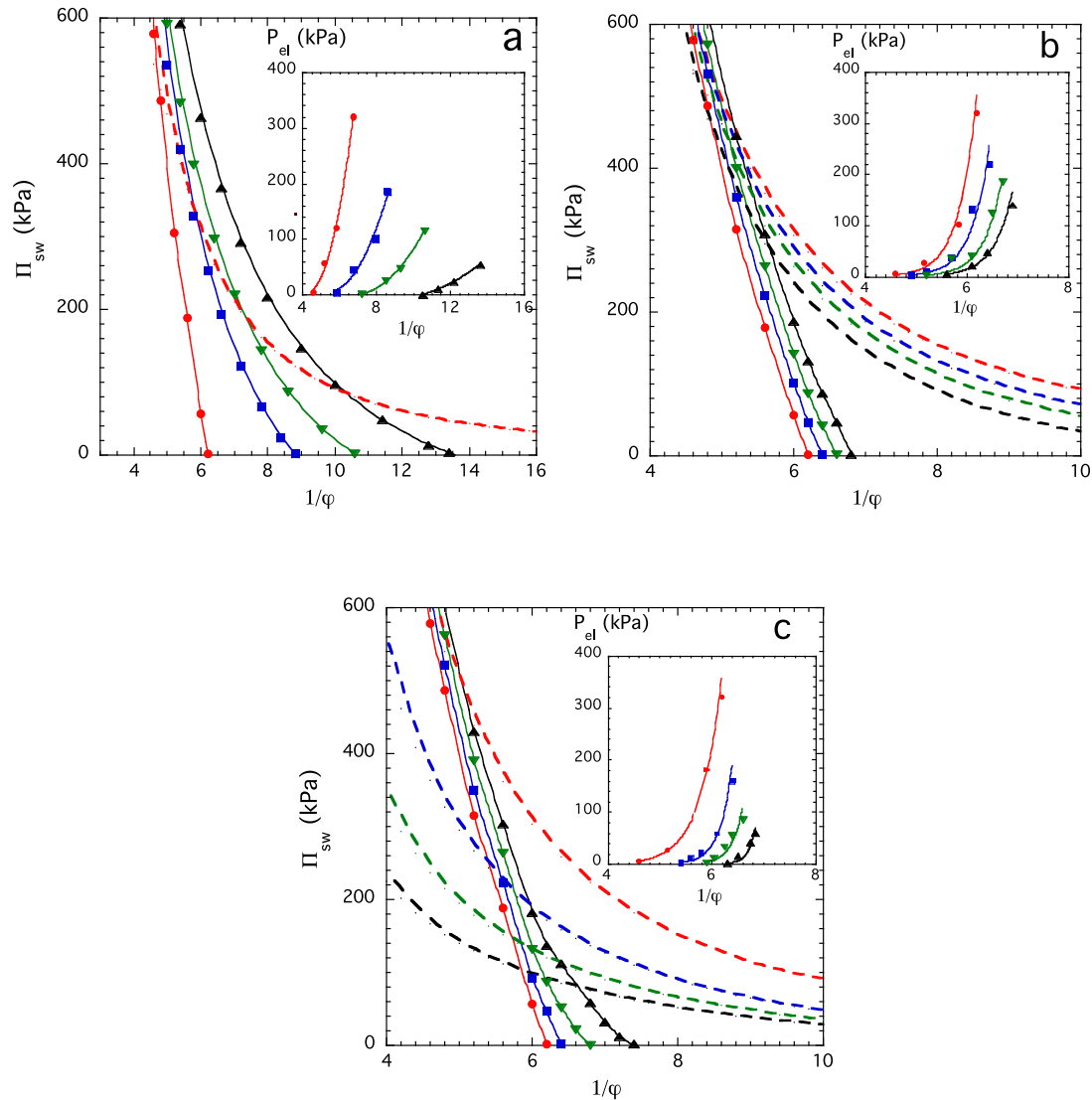
Figure 3. Π_{sw} vs $1/\varphi$ plots for PVA/PAA composite gels. a. PVA/PAA gels with varying network stiffnesses (continuous curves), PAA gel (dashed curve). Symbols: ▲ PVA1/PAA1, ▼ PVA2/PAA1, ■ PVA3/PAA1 ● PVA4/PAA1. b. PVA4/PAA gels containing PAA particles of varying nominal crosslink densities: ● 0.03, ■ 0.06, ▼ 0.09, ▲1.20 %). Dashed curves: Π_{sw} vs $1/\varphi$ plots for PAA gels with varying crosslink densities (red: 0.03%, blue: 0.06%. green: 0.09%, black: 1.2%). c. PVA4/PAA gels containing PAA particles swollen in $CaCl_2$ solutions of varying concentrations: ● 0 mM, ■ 0.1 mM, ▼ 0.2 mM, ▲ 0.3 mM. Dashed curves: Π_{sw} vs $1/\varphi$ plots for PAA gels in $CaCl_2$ solutions of varying concentrations (red: 0 mM, blue: 0.1 mM, green: 0.2 mM, black: 0.3 mM). Insets: tensile stress (P_{el}) vs $1/\varphi$ plots for the same gels shown in the main figures.

There is an important conceptual difference between the swelling behavior of the pure PVA gels and the PVA/PAA composite gels. In the latter, the PAA particles are trapped in the PVA matrix. As the swelling degree of the PAA increases the PVA matrix

becomes inflated (see Figure 2), however, the PVA matrix limits the swelling of the PAA. So when the composite gel is fully swollen ($\Pi_{sw} = 0$), the PVA matrix is in tension. The tensile stress of the inflated gel is defined as

$$P_{el} = \Pi_{PAA} - \Pi_{sw} \tag{14}$$

When $\Pi_{sw} = \Pi_{PAA}$ the PVA and PAA gels are in equilibrium and the tensile stress $P_{el} = 0$. The inset in Figure 3a illustrates that the pre-stress P_{el} increases with increasing network stiffness and reaches a maximum, $P_{el}{}^{max}$, at the fully swollen state, i.e., at $\Pi_{sw} = 0$. Clearly, matrix stiffness plays multiple roles in controlling the osmotic properties of composite gels: (i) it defines the tensile stress that develops in the inflated system, and (ii) it limits the swelling of the encapsulated gel particles.

We analyzed P_{el} by fitting an exponential function to the data as predicted by the Fung model. The agreement with the prediction of the semi-flexible chain network model of Lin et al.[98] (or equivalently the "Fung model") is surprisingly good since we tend to think of PVA and PAA as being relatively flexible polymers. However, it is well documented in the literature that microcrystalline domains formed in the freeze-thaw process can significantly increase the stiffness of the PVA network. Furthermore, PAA inflates the PVA matrix thus increasing the overall rigidity of the composite system.

Determination of the optimal crosslink density of PAA particles to maximize gel strength is not obvious although considering the two extremes of weak and dense crosslinking suggests that such an optimum exists. Weakly crosslinked PAA exhibits high swelling pressure that eventually destabilizes and destroys the PVA matrix. On the other hand, the limited swelling of densely crosslinked PAA particles may not be sufficient to inflate the PVA gel.

Figure 3b shows the influence of the crosslink density of the PAA particles on the swelling pressure of PVA/PAA composite gels. Increasing crosslink density progressively reduces the swelling of the PAA particles, and shifts the Π_{sw} vs $1/\varphi$ plots toward lower swelling pressures. The inset in Figure 2b illustrates that (i) P_{el} in the present system gradually decreases with increasing crosslink density of the PAA and (ii) the P_{el} vs $1/\varphi$ plots are nearly parallel. This finding implies that the main effect of the

18

crosslink density of PAA is defining P_{el}^{max}.

In Figure 3c are shown the effect of Ca^{2+} ions on the swelling pressure of PVA/PAA composite gels. This experiment aimed to model the influence of fixed charge density on the osmotic properties. The NaCl concentration was kept constant ($c_{NaCl} = 100$ mM) and the $CaCl_2$ concentration was varied in the range $0 < c_{CaCl2} \leq 0.3$ mM. [At higher $CaCl_2$ concentration ($c_{CaCl2} > 0.8$ mM) the PAA gels collapse.] Figure 3c indicates that the ionic environment strongly affects the shape of the PAA curves: both the numerical values of Π_{sw} as well as the slope of the Π_{sw} vs $1/\varphi$ plots strongly decreases with increasing $CaCl_2$ concentration. Clearly, Ca^{2+} ions reduce the effective charge on the polymer chains, i.e., the repulsive electrostatic interactions between the polymer molecules. This effect resembles that of increasing crosslink density, however, the underlying molecular mechanism is entirely different. Ca^{2+} ions do not form crosslinks between neighboring PAA chains as demonstrated in the literature.[71,72,76]

In summary, in "uninflated" gels the elastic pressure primarily arises from entropic retractive forces, which develop as the network swells and the number of degrees of freedom of the chains is reduced. At equilibrium the decrease of the free energy due to mixing of the polymer and solvent molecules is balanced by the free energy increase due to stretching of the network chains. In this physical situation, the osmotic mixing pressure of the crosslinked polymer is always greater than the swelling pressure of the gel, and the elastic pressure Π_{el} decreases with increasing swelling degree as shown in Figure 1. By contrast, for gels inflated by swelling particle inclusions, the reduction of the elastic pressure is compensated by the tensile stress developing in the matrix due to swelling of the trapped gel particles. Consequently, P_{el} gradually increases as the swelling degree increases. The Π_{sw} vs $1/\varphi$ curve of the PVA matrix intercepts that of the PAA gel. At their intersection $\Pi_{sw}^{composite} = \Pi_{sw}^{PAA}$ and $P_{el} = 0$. The position of the intersection and the magnitude of P_{el} depend on (i) the stiffness of the PVA network, (ii) the crosslink density of the PAA particles, and (iii) the Ca^{2+} ion concentration of the equilibrium salt solution. With increasing swelling degree P_{el} increases and reaches a maximum P_{el}^{max} when the gel is fully swollen. P_{el}^{max} increases with the stiffness of the PVA matrix, and decreases with increasing crosslink density and decreasing effective

19

charge density of the PAA particles. $P_{el}{}^{max}$ defines the load bearing ability of composite gels.

Small angle neutron scattering

Although osmotic swelling pressure measurements provide invaluable insight into the thermodynamics of composite hydrogels they do not provide information on the organization of the polymer components. SANS allows us to probe the structure of composite gels over a broad range of length scales and quantify the interactions that govern the macroscopic thermodynamic properties.

Figure 4 shows typical SANS profiles of PVA and PAA gels. Data are presented for two PVA gels (PVA1 and PVA3) differing in network stiffness. The scattering curves of these PVA gels exhibit similar qualitative features. In PVA1 two plateaus are clearly distinguishable; one in the intermediate q regime and the other one at low q. In both PVA samples the shoulder at high q corresponds to the Ornstein–Zernike thermal contribution to the scattering signal, while the excess scattering at low q can be attributed to structural inhomogeneities (large polymer clusters, etc.) frozen in by the crosslinks. The scattering profiles show that the intensity arising from inhomogeneities increases with increasing stiffness. In PVA3 the low q plateau is less pronounced indicating that the size of the inhomogeneities varies nearly continuously over the length scale range from 10 Å to approximately 500 Å explored in the SANS experiment. It is known that PVA gels contain microcrystallites, which are also expected to contribute to the scattering intensity, since they modify the local polymer concentration. At high q the PVA1 and PVA3 signals are practically indistinguishable indicating that the local structure of the PVA chains is not influenced by the presence of larger scale objects.

20
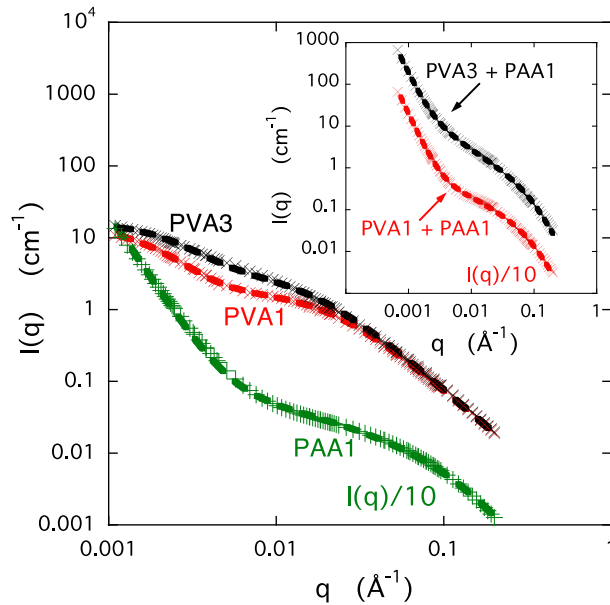
Figure 4. SANS profiles of PVA and PAA gels. Continuous curves through the data points are least squares fits of eq. 15 (PVA gels) and eq. 16 (PAA gel). The intensity of the PAA curve is divided by 10 for clarity. Inset: Comparison of the SANS response of composite gels with the sum of the SANS curves of the components. The intensity of the PVA1+PAA1 curve is divided by 10 for clarity.

The dashed curves through the PVA data points are least squares fits of

$$I(q) = \frac{A_1}{\left(1+q^2\xi^2\right)} + \frac{A_2}{\left(1+q^2\Xi^2\right)} \tag{15}$$

where A_1 and A_2 are constants. The values of A_1, A_2, ξ and Ξ listed in Table 2 show that the intensities as well as the characteristic lengths increase with increasing network stiffness.

21

Table 2.

Fitting parameters to the SANS profiles of PVA and PAA gels

Sample	A_1 (cm^{-1})	A_2 (cm^{-1})	ξ (Å)	Ξ (Å)	m
PVA1	1.75	12.9	46	308	--
PVA3	3.2	13.6	62	397	--
PAA1	0.3	2x10^{-7}	23	---	-3.2

The scattering response of the PAA gel significantly differs from that of the PVA gels. At low q (< 0.08 Å^{-1}) a power law behavior is observed characteristic of scattering from large clusters. This behavior is typical of polyelectrolyte gels and solutions.[24,26,76,103-105] Because of the absence of a shoulder in this region, the size of the clusters cannot be estimated from the SANS profile. At low q the slope varies as $m \approx -3.2$. Such a power-law behavior indicates that in the low q regime the PAA gel exhibits fractal-like behavior. As discussed earlier for scattering from objects with fractal surface, the power law exponent is related to the fractal dimension. The slope of the log-log plot in Figure 4 yields $D_s \approx 2.8$. At intermediate q a plateau region is distinguishable, which is described by the first term of equation 16. The dashed curve is fit to the equation

$$I(q) = \frac{A_1}{\left(1+q^2\xi^2\right)} + A_2 q^{-m} \tag{16}$$

The fitting parameters are displayed in the last row of Table 2.

To glean additional information about the interaction between the two polymers we also made SANS measurements on composite gels. SANS reveals the length scales over which the components interact and provides information on the nature and the strength of their interaction, and the changes occurring in the underlying molecular and supramolecular structure. In the inset in Figure 4 the SANS response of PVA/PAA

composite gels are compared with the sum of the SANS profiles of the components. The shape of the measured and calculated curves is similar, indicating the absence of significant interaction between the two polymer gels. This finding implies that the two crosslinked polymers in the PVA/PAA composite gel can be treated as independent entities.

Biomedical relevance of load bearing composite gels

Swelling pressure of PVA/PAA composite gels and cartilage specimen

In this section we compare the osmotic response of the present composite gels with osmotic swelling pressure data reported for cartilage specimens in the literature.[18] The authors determined the tensile stress of the collagen matrix P_{el} as a function of hydration for healthy human cartilage samples, and for cartilage from an osteoarthritic (OA) joint (Figure 5a). In healthy cartilage the P_{el} *vs* hydration curves exhibited a steep increase with increasing hydration. High PG concentration, high charge density, and high Π_{PG} reflect the large stiffness of the collagen matrix. During loading of healthy cartilage, changes in tissue swelling are relatively small. By contrast, the P_{el} *vs* hydration curve for the OA specimen was significantly less steep and displaced to higher hydrations, indicating that in OA cartilage the collagen network is much weaker (i.e., more flaccid), and the tissue swells more. Because of its high water content the OA cartilage cannot develop high PG concentration and its load bearing capacity is limited (Figure 5a inset).

Figure 5b illustrates that PVA/PAA composite hydrogels exhibit qualitatively similar osmotic response to cartilage tissue. The PVA4/PAA1 gel mimics the healthy cartilage, while the osmotic behavior of the OA cartilage is close to that of the PVA2/PAA1 gel. In the latter system the stiffness of the PVA gel is about half of the PVA component in the PVA4/PAA1 gel. This reduction in the stiffness of the matrix polymer reproduces the reduced swelling pressure of the OA specimen.[18,106] The biomimetic model describes both the shape of the cartilage curves and the numerical values of the experimental swelling pressure.
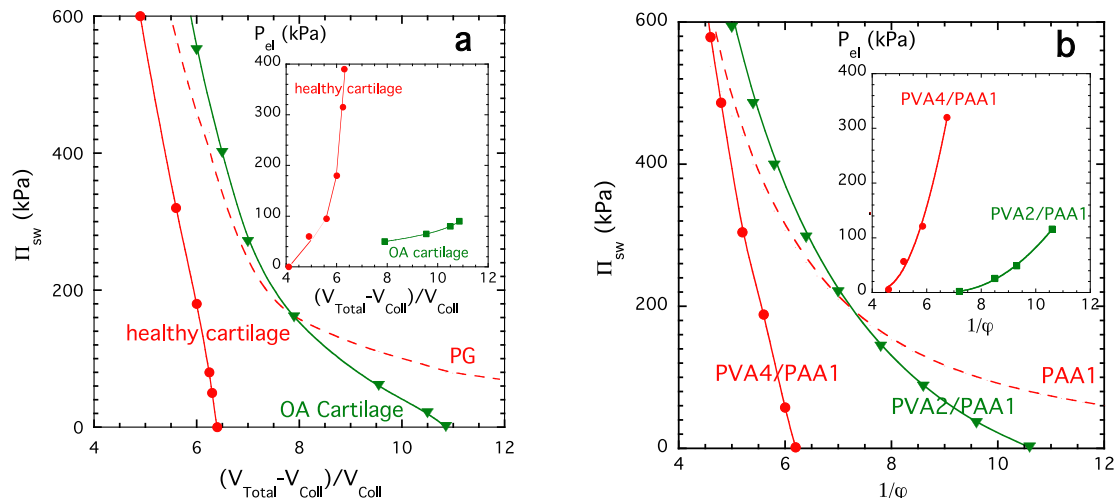
Figure 5. Comparison between the swelling behavior of cartilage samples (figure a) and PVA/PAA composite gels (figure b). In figure a the x-axis represents the hydration of the cartilage, V_{Total} is the total tissue volume and V_{Coll} is the volume of the collagen Insets: tensile stress vs hydration curves.

Tailoring the osmotic properties of implants

Recent advances in tissue engineering have enabled remarkable progress in controlling the properties of implants. There are numerous structural and functional requirements that the engineered tissue should meet to be clinically applicable as an ECM substitute. One of the biggest challenges is the integration of the engineered construct with native tissues. The biomechanical properties of the implant (e.g., swelling pressure, compressive, tensile, and shear properties) should match as closely as possible the properties of the host tissue in which it is implanted. Matching the osmotic and mechanical properties at the site of implantation and perfect integration of the implant with the surrounding tissue insures that in the course of the healing process tissue regeneration is not compromised by mechanical failure. Therefore, knowing the osmotic properties of the implant is critically important for tailoring its biomechanical/biochemical properties to develop successful regenerative medicine strategies.

Engineering pre-stressed tissue implants

The aim of cartilage tissue engineering is the creation of a replacement tissue to restore normal joint function. Although, engineered cartilage exhibits histological and biochemical characteristics similar to those of the native tissue, the implants fail to

possess suitable mechanical properties.[107,108] In previous studies the importance of tissue inflation has been largely overlooked. However, pre-stress governs the load bearing properties and is a critically important factor for designing and engineering cartilage repair implants. The load bearing ability depends not only on the amounts of collagen and PGs but also on their structural organization. The ability of collagen to resist tension ultimately provides the shear stiffness of the tissue. The role of PG assemblies is to inflate the collagen matrix but PGs alone do not improve tissue stiffness. The tensile stress developing in the collagen network ensures that the tissue operates in the inflated state (i.e., at increased matrix stiffness) and exhibits enhanced load bearing properties. High collagen content is a basic requirement for load bearing. There are biochemical methods to control the collagen to aggrecan ratio. For example, catabolic enzymes (e.g., chondroitinase, hyaluronidase) deplete PGs.[109,110] Suppression of GAG synthesis may be beneficial for engineering an inflated matrix, thus improving the mechanical properties of the implant. However, reducing the PG concentration also reduces the pre-stress, and ultimately the stiffness of the tissue. Our biomimetic model makes it possible to systematically investigate the effect of different factors and develop strategies to optimize the load bearing properties of cartilage implants.

Conclusions

Systematic osmotic swelling pressure measurements are reported for a composite gel system which mimics articular cartilage, consisting of a crosslinked PVA hydrogel containing PAA gel particles. The measurements were made in near-physiological salt solutions. The effects of the stiffness of the PVA gel, the crosslink density of the PAA and the Ca^{2+} ion concentration were studied.

In PVA/PAA composite gels the PAA component inflates the PVA matrix and enhances the load bearing ability of the system. The swollen PAA particles generate a tensile stress in the matrix, which increases as the gel adsorbs more liquid. The functional form of P_{el} can be described by the Fung-model derived for stiff polymers.

SANS measurements made on PVA/PAA composite gels indicate the absence of considerable interaction between the two polymeric components.

The osmotic behavior of gels inflated by swollen inclusions is qualitatively

different from that of ordinary (noninflated) gels. In the latter gels the osmotic mixing pressure of the crosslinked polymer always exceeds the swelling pressure of the gel, and the elastic pressure gradually decreases as the network swells. By contrast, in inflated gels the swelling pressure *vs.* swelling degree curve of the enclosed particles (PAA) intercepts that of the composite gel. At the intersection $\Pi_{sw}^{composite} = \Pi_{sw}^{PAA}$ and $P_{el} = 0$. P_{el} steeply increases with the swelling degree and it reaches a maximum P_{el}^{max} when the composite gel is fully swollen ($\Pi_{sw} = 0$). The position of the intersection and P_{el}^{max} is defined by (i) the stiffness of the PVA network, (ii) the crosslink density of the PAA particles, and (iii) the Ca^{2+} ion concentration of the equilibrium solution.

A comparison has been made between the osmotic response of PVA/PAA composite gels and healthy and osteoarthritic cartilage specimens. It is found that the composite gels satisfactorily reproduce not only the shape of the cartilage curves but also the numerical values reported for the swelling pressure of cartilage.

References

1. B.S. Kim and D.J. Mooney, Development of biocompatible synthetic extracellular matrices for tissue engineering. *Trends Biotechnol.* 1998, **16**, 224–230.

2. N.E. Federovich, J. Alblas, J.R. Dewijn, W.E. Hennink, A.J. Verbout and W.J.A. Dhert, Hydrogels as extracellular matrices for skeletal tissue engineering: state-of-the-art and novel application in organ printing. *Tissue Eng.* 2007, **13**, 1905–1925.

3. A. Khademhosseini, R. Langer, J. Borenstein, and J.P. Vacanti, Microscale technologies for tissue engineering and biology. *Proc Natl Acad Sci.* 2006, **103**, 2480–2487.

4. J.B. Leach and C.E. Schmidt, Characterization of protein release from photocrosslinkable hyaluronic acid-polyethylene glycol hydrogel tissue engineering scaffolds. *Biomaterials*. 2005, **26**, 125–135.

5. N. Peppas, J.Z. Hilt, A. Khademhosseini and R. Langer, Hydrogels in biology and medicine. *Adv Mater*. 2007, **18**, 1–17.

6. K.S. Anseth, C.N. Bowman and L. Brannon-Peppas, Mechanical properties of hydrogels and their experimental determination. *Biomaterials*. 1996, **17**, 1647–1657.

7. K. Jakab, B. Damon, A. Neagu, A. Kachurin and G. Forgacs, Three-dimensional tissue constructs built by bioprinting. *Biorheology*. 2006, **43**, 509–513.

8. M.S. Hahn, J.S. Miller and J.L. West, Three-dimensional biochemical and biomechanical patterning of hydrogels for guiding cell behavior. *Adv Mater*. 2006, **18**, 2679–2684.

9. K.Y. Lee and D.J. Mooney, Hydrogels for tissue engineering. *Chem Rev*. 2001, **101**, 1869–1877.
.
10. M.W. Tibbitt and K.S. Anseth, Hydrogels as extracellular matrix mimics for 3D cell culture. *Biotechnol Bioeng*. 2009, **103**, 655–663.

11. Y. Du, E. Lo, S. Ali, and A. Khademhosseini, A. Directed assembly of cell-laden microgels for fabrication of 3D tissue constructs. *Proc Natl Acad Sci USA,* 2008, **105**, 9522–9527.

12. B.V. Slaughter, S.S. Khurshid, O.Z. Fisher, A. Khademhosseini and N.A. Peppas, Hydrogels in regenerative medicine. *Adv Mater*. 2009, **21**, 3307–3329.

13. V.C. Mow, and C.T.Hung, in *Basic Biomechanics of the Musculoskeletal System*, eds. M. Nordin and V. H. Frankel, Lippincott Williams & Wilkins, Philadelphia, PA, 2001.

14. V.C. Mow, W. Zhu and A. Ratcliffe, A. in *Basic Orthopedic Biomechanics*, eds. V. C. Mow and W. C. Hayes, Raven Press,, New York, NY, 1991.

15. L. Ng, A.J. Grodzinsky, P. Patwari, J.Sandy, A. Plaas and C. Ortiz, Individual cartilage aggrecan macromolecules and their constituent glycosaminoglycans visualized via atomic force microscopy. *Journal of Structural Biology*, 2003, **143**, 242-257.

16. A.G. Ogston, in *Chemistry and Molecular Biology of the Intercellular Matrix*, ed. E. A. Balazs, Academic Press, London, 1970, vol. 3, pp. 1231-1240.

17. A. Maroudas and C. Bannon, Measurement of swelling pressure in cartilage and comparison with the osmotic-pressure of constituent proteoglycans. *Biorheology*, 1981, **18**, 619-632.

18. P.J. Basser, R. Schneiderman, R.A. Bank, E. Wachtel and A. Maroudas, A. Mechanical properties of the collagen network in human articular cartilage as measured by osmotic stress technique. *Archives of Biochemistry and Biophysics*, 1998, **351**, 207-219.

19. R.Iozzo, R .*Proteoglycans: Structure, Biology, and Molecular Interactions*, Marcel Dekker, New York 2000.

20. J. Kisiday, M. Jin, B. Kurz, H. Hung, C. Semino, S. Zhang and A.J. Grodzinsky, Self-assembling peptide hydrogel fosters chondrocyte extracellular matrix production and cell division: Implications for cartilage tissue repair. *Proceedings of the National Academy of Sciences of the United States of America*, 2002, **99**, 9996-10001.

21. F**.** Horkay, P.J. Basser, A.M. Hecht and E. Geissler, Gel-like Behavior in Aggrecan Assemblies, *Journal of Chemical Physics* 2008, **128**, 135103.

22. P.L. Chandran, P.L. and F. Horkay, Aggrecan, an Unusual Polyelectrolyte: Review of Solution Behavior and Physiological Implications. *Acta Biomaterialia* 2012, **8**, 3–12.

23. F. Horkay, P. J. Basser, A. M. Hecht and E. Geissler, *Macromolecular Symposia*, 2011, **306-307**, 11-17.

24. F. Horkay, P.J. Basser, D.J. Londono, A.M. Hecht and E. Geissler, Ions in Hyaluronic Acid Solutions, *Journal of Chemical Physics* 2009, **131**, 184902.

25. F. Horkay, Ion Polymer Interactions in DNA Solutions and Gels. *Macromol. Symp.* 2013, **329**, 19–26.

26. F. Horkay, P.J. Basser, A.M. Hecht and E. Geissler, Chondroitin Sulfate in Solution: Effects of Mono- and Divalent Salts. *Macromolecules* 2012, **45**, 2882−2890.

27. J.W. Kim, A.S. Utada, A.Fernańdez-Nieves, Z. Hu and D. Weitz, Fabrication of monodisperse gel shells and functional microgels in microfluidic devices. *Angew. Chem. Int. Ed.* 2007, **46**, 1819−1822.

28. C.J. Cheng, L.Y. Chu, P.W. Ren, J. Zhang and L. Hu, Preparation of monodisperse thermo-sensitive poly(N-isopropylacrylamide) hollow microcapsules. *J. Colloid Interface Sci.* 2007, **313**, 383−388.

29. R.K. Shah, J.W. Kim, J.J. Agresti, D.A. Weitz, L.Y. Chu, Fabrication of monodisperse thermosensitive microgels and gel capsules in microfluidic devices. *Soft Matter* 2008, **4**, 2303−2309.

30. N. Welsch, A. Wittemann and M. Ballauff, Enhanced activity of enzymes immobilized in thermoresponsive core-shell microgels. *J. Phys. Chem. B*. 2009, **113**, 16039−16045.

31. A. Fernandez, H.M. Wyss, J. Mattsson and D.A. Weitz, Microgel Suspensions: Fundamentals and Applications; Wiley-VCH: Weinheim, 2011.

32. N. Welsch, A.L. Becker, J. Dzubiella and M. Ballauff, M. Core-shell microgels as "smart" carriers for enzymes. *Soft Matter* 2012, **8**, 1428− 1436.

33. Y.Y. Li, and S.Q. Zhou, A simple method to fabricate fluorescent glucose sensor based on dye-complexed microgels. *Sens. Actuator, B*, 2013, **177**, 792−799.

34. E.B. Hunziker, Articular cartilage repair: Basic science and clinical progress. A review of the current status and prospects. *Osteoarthr. Cartil.* 2002, **10**, 432–463.

35. M.S. Bae, D.H. Yang, J.B. Lee, D.N. Heo, Y.D. Kwon, I.C. Youn, K. Choi, J.H. Hong, G.T. Kim, Y.S. Choi, et al. Photo-cured hyaluronic acid-based hydrogels containing simvastatin as a bone tissue regeneration scaffold. *Biomaterials* 2011, **32**, 8161–8171.

36. J.L.C. Van Susante, J.Pieper, P. Buma, T.H. van Kuppevelt, H. van Beuningen, P.M. van der Kraan, J.H. Veerkamp, W.B. van den Berg and R.P.H. Veth, Linkage of chondroitin-sulfate to type I collagen scaffolds stimulates the bioactivity of seeded chondrocytes in vitro. *Biomaterials* 2001**, 22**, 2359–2369.

37. D.L. Nettles, T.P. Vail, M.T. Morgan, M.W. Grinstaff and L.A. Setton, Photocrosslinkable hyaluronan as a scaffold for articular cartilage repair. *Ann. Biomed. Eng.* 2004, **32**, 391–397.

38. G.D. Nicodemus and S.J. Bryant, Cell encapsulation in biodegradable hydrogels for tissue engineering applications. *Tissue Eng. B Rev.* 2008, **14**, 149–165.

39. J.K. Katta, M. Marcolongo, A.M. Lowman and K.A. Mansmann, Friction and wear behavior of poly(vinyl alcohol)/poly(vinyl pyrrolidone) hydrogels for articular cartilage replacement. *J Biomed Mater Res A*, 2007, **83**, 471–479.

40. C. Grant, P. Twigg, A. Egan, A. Moody, A. Smith, and D. Eagland, Poly(vinyl alcohol) hydrogel as a biocompatible viscoelastic mimetic for articular cartilage. *Biotechnol Prog.* 2006, **22**, 1400–1406.

41. A. Joshi, G. Fussell, J. Thomas, A. Hsuan, A.M. Lowman and A. Karduna, Functional compressive mechanics of a PVA/PVP nucleus pulposus replacement. *Biomaterials* 2006, **27**, 176–184.

42. B.H. Wang and G. Campbell, Formulations of polyvinyl alcohol cryogel that mimic the biomechanical properties of soft tissues in the natural lumbar intervertebral disc. *Spine* 2009, **34**, 2745–2753.

43. R, Ma, D. Xiong, F. Miao, J. Zhang and Y. Peng, Novel PVP/PVA hydrogels for

articular cartilage replacement. *Mater Sci Eng C: Mater*. 2009, **29**, 1979–1983.

44. M.J. Allen, J.E. Schoonmaker, T.W Bauer, P.F. Williams, P.A. Higham and H.A. Yuan, Preclinical evaluation of a poly(vinyl alcohol) hydrogel implant as a replacement for the nucleus pulposus. *Spine* 2004, **29**, 515–523.

45. D.W. Yin, F. Horkay, J.F. Douglas and J.J. de Pablo, Molecular simulation of the swelling of polyelectrolyte gels by monovalent and divalent counterions. *J Chem Phys*. 2008, **129**, 154902.

46. M. Kobayashi, Y. Chang and M. Oka. A two year in vivo study of polyvinyl alcohol hydrogel (PVA-H) artificial meniscus. *Biomaterials* 2005, **26**, 3243–3248.

47. J.L. Holloway, A.M. Lowman and G.R. Palmese, Mechanical evaluation of poly(vinyl alcohol) based fibrous composites as biomaterials for meniscal tissue replacement. *Acta Biomater.* 2010, **6**, 4716–4724.

48. J. Beyerlein and A.B, Imhoff, Salucartilage a new synthetic cartilage replacement for the arthroscopic treatment of focal osteonecrosis. *Arthroscopy* 2003, **16**, 34–39.

49. M.I. Baker, S.P. Walsh, Z. Schwartz and B.D. Boyan, B.D. A review of polyvinyl alcohol and its uses in cartilage and orthopedic applications. *J Biomed Mater Res Part B* 2012, **100B**, 1451–1457.

50. T. Tanigami, Y. Nakashima, K. Murase, H. Suzuki, K. Yamaura and S. Matsuzawa,. High strength and high modulus poly(vinyl alcohol) by the gel ageing method. *J Mater Sci.* 1995, **30**, 5110–5120.

51. P. Willcox, D. Howie, K. Schmidt-Rohr, D. Hoagland, S. Gido and S. Pudjijanto , Microstructure of poly(vinyl alcohol) hydrogels produced by freeze/thaw cycling. *J Polym Sci: Polym. Phys.* 1999, **37**, 3438–3454.

52. C. Hassan, N.A. Peppas, Structure and applications of poly(vinyl alcohol) hydrogels produced by conventional crosslinking or by freezing/thawing methods. *Adv. Polym. Sci.* 2000, **153**, 37–66.

53. R. Ricciardi, F. Auriemma, C. Gaillet, and C. De Rosa, Investigation of the crystallinity of freeze/thaw poly(vinyl alcohol) hydrogels by different techniques. *Macromolecules* 2004, **37**, 9510–9516.

54. R. Ricciardi, F. Auriemma, C. De Rosa and F. Laupretre, X-ray diffraction analysis of poly(vinyl alcohol) hydrogels, obtained by freezing and thawing techniques. *Macromolecules* 2004, **37**, 1921–1927.

55. R. Hernandez, A. Sarafian and D. Lopez, Viscoelastic properties of poly(vinyl alcohol) hydrogels and ferrogels obtained through freezing–thawing cycles. *Polymer*

2004, **46**, 5543–5549.

56. D.Z. Yang, Y. Jin, G.P. Ma, X.M. Chen, F.M. Lu and J. Nie, Fabrication and characterization of chitosan/PVA with hydroxyapatite biocomposite nanoscaffolds. *J. Appl. Polym. Sci.* 2008, **110**, 3328–3335.

57. W.Y. Choi, H.E. Kim and S.Y. Oh, Synthesis of poly(ε-caprolactone)/hydroxyapatite nanocomposites using in-situ co-precipitation. *Mater. Sci. Eng., C*, 2010, **30**, 777–780.

58. X.M. Shi, S.M. Xu and J.T. Lin, Synthesis of SiO2-polyacrylic acid hybrid hydrogel with high mechanical properties and salt tolerance using sodium silicate precursor through sol-gel process. *Mater. Lett.* 2009, **63**, 527–529.

59. E. Wenk, A.J. Meinel A. and S. Wildy, Microporous silk fibroin scaffolds embedding PLGA microparticles for controlled growth factor delivery in tissue engineering, *Biomaterials*, 2009, **30**, 2571–2581.

60. C.S. Chen and D.E. Ingber, Tensegrity and Mechanoregulation: from Skeleton to Cytoskeleton, Osteoarthritis and Cartilage, 1999, **7**, 81-94.

61. P.J. Flory and J. Rehner, Jr. Statistical mechanics of cross-linked polymer networks II Swelling. *J. Chern. Phys.* 1943, **11**, 521-526.

62. P.J. Flory, *Principles of Polymer Chemistry,* Cornell University, Ithaca, NY, 1953.

63. L.R.G. Treloar, *The Physics of Rubber Elasticity,* Clarendon, Oxford.1975.

64. M. Nagy and F. Horkay, A Simple and Accurate Method for the Determination of Solvent Activity in Swollen Gels, *Acta Chim. Acad. Sci. Hung.* **1980**, 104, 49-61.

65. F. Horkay and M. Zrinyi, Studies on Mechanical and Swelling Behavior of Polymer Networks Based on the Scaling Concept, *Macromolecules*, 1982, **15**, 1306-1310.

66. R.W. Brotzman and B.E. Eichinger, Swelling of model poly(dimethylsiloxane) networks. *Macromolecules*, 1983, **16**, 1131–1136.

67. F. Horkay, I. Horkayne-Szakaly and P.J. Basser, Measurement of the Osmotic Properties of Thin Polymer Films and Biological Tissue Samples. *Biomacromolecules* 2005, **6**, 988-993.

68. G.B. McKenna, K.M. Flynn and Y. Chen, Experiments on the elasticity of dry and swollen networks - implications for the Frenkel-Flory-Rehner hypothesis. *Macromolecules* 1989, **22**, 4507-4512.

69. F. Horkay, E. Geissler, A.M. Hecht and M. Zrinyi, Osmotic Swelling of Poly(vinyl acetate) Gels at the θ Temperature, *Macromolecules*, 1988, **21**, 2589-2594.

70. S.R. Eisenberg and A.J. Grodzinsky, Swelling of articular cartilage and other connective tissues: electromechanochemical forces. *J. Orthop. Res.* 1985, **3**, 148-159.

71. F. Horkay, I. Tasaki and P. Basser, Osmotic swelling of polyelectrolyte hydrogels in physiological salt solutions, *Biomacromolecules*, 2000, **1**, 84-90.

72. F. Horkay, I. Tasaki and P. Basser, Effect of monovalent-divalent cation exchange on the swelling of polyacrylate hydrogels in physiological salt solutions. *Biomacromolecules*, 2001, **2**, 195-199.

73. F. Horkay, P.J. Basser, A.M. Hecht and E. Geissler, Comparison between neutral gels and neutralized polyelectrolyte gels in the presence of divalent cations. *Macromolecules* 2001, **34**, 4285-4287.

74. F. Horkay, P.J. Basser, A.M. Hecht and E. Geissler, Structural investigations of a neutralized polyelectrolyte gel and an associating neutral hydrogel. *Polymer* 2005, **46**, 4242-4247.

75. F. Horkay and P.J. Basser, Osmotic observations on chemically cross-linked DNA gels in physiological salt solutions. *Biomacromolecules* 2004, **5**, 232-237.

76. F. Horkay, P.J. Basser, A.M. Hecht and E. Geissler, Effect of Calcium/Sodium Ion Exchange on the Osmotic Properties and Structure of Polyelectrolyte Gels. *Proceedings of the Institution of Mechanical Engineers, Part H: Journal of Engineering in Medicine*, 2015, **229**, 895-904.

77. F.T. Wall, Statistical thermodynamics of rubber. *J. Chem. Phys,* 1942, **10**, 132-134.

78. P.J. Flory, Network structure and the elastic properties of vulcanized rubber. *Chem. Rev.* 1944, **35**, 51-75.

79. F.T. Wall and P.J. Flory, Statistical thermodynamics of rubber elasticity. *J. Chem. Phys.* 1951, **19**, 1435-1439.

80. H.M. James and E. Guth, Theory of the elastic properties of rubber. *J. Chem. Phys.* 1943, **11**, 455-481.

81. H.M. James and E. Guth, Theory of the increase in rigidity of rubber during cure. *J. Chem. Phys.* 1947, **15**, 669-683.

82. H.M. James and E. Guth, Simple presentation of network theory of rubber, with a discussion of other theories. *J. Polym. Sci.* 1949, **4**, 153-182.

83. R.J. Gaylord and J.F. Douglas, Rubber elasticity - A scaling approach. *Polym. Bull.* 1987, **18**, 347-354.

84. R.J. Gaylord and J.F. Douglas, The localization model of rubber elasticity. *Polym. Bull.* 1990, **23**, 529-533.

85. J.F. Douglas and G.B. McKenna, The effect of swelling on the elasticity of rubber - Localization model description. *Macromolecules,* 1993, **26***,* 3282-3286.

86. W.H. Han, F. Horkay and G.B. McKenna, Mechanical and Swelling Behaviors of Rubber: A Comparison of Some Molecular Models with Experiment. *Mathematics and Mechanics of Solids.* 1999, **4**, 139-167.

87. T.A. Vilgis, F. Boue and S.F. Edwards, in Moelcular Basis of Polymer Network 1988: Workshop Proceedings, edited by A. Baumgartner and C. E. Picot (Springer-Verlag, Berlin, 1989).

88. Y.C. Fung, *Biomechanics: Mechanical Properties of Living Tissues*, Springer-Verlag, New York, 1993.

89. L.S. Ornstein and F. Zernike, Acculental deviations of density and opalescence at the critical point of a simple substance. *Proc Sect Sci K Med Akad Wet.* 1914, **17**, 793-806.

90. T. Tanaka, L.O. Hocker and G.B. Benedek, Spectrum of light scattered from a viscoelastic gel. *J Chem Phys*. 1973, **59**, 5151–5156.

91. F. Horkay, A.M. Hecht, S. Mallam, E. Geissler and A.R. Rennie, Macroscopic and microscopic thermodynamic observations in swollen polyvinylacetate networks. *Macromolecules* 1991, **24**, 2896–2902.

92. S. Mallam, F. Horkay, A.M. Hecht and E. Geissler, Scattering and swelling properties of inhomogeneous polyacrylamide gels. *Macromolecules* 1989, **22**, 3356–3361.

93. F. Horkay, W. Burchard, E. Geissler and A.M. Hecht, Thermodynamic Properties of Poly(vinyl alcohol) and Poly(vinyl alcohol-vinyl acetate) Hydrogels. *Macromolecules* 1993, **26***,* 1296-1303.

94. P. Debye and A.M. Bueche, Scattering by an inhomogeneous solid. *J Appl Phys*. 1949, **20**, 518–536.

95. H. Vink, Precision measurements of osmotic pressure in concentrated polymer solutions. *Eur. Polym. J.* 1971, **7**, 1411–1419.

96. NIST Cold Neutron Research Facility. NG3 and NG7 30-meter SANS Instruments Data Acquisition Manual; January 1999.

97. J. Brandrup and E.H. Immergut,{editors), Polymer handbook. 3rd edition. NewYork/Chichester/Brisbane/Toronto/Singapore: John Wiley & Sons 1989.

98. D.C. Lin, J.F. Douglas and F. Horkay, Development of minimal models of the elastic properties of flexible and stiff polymer networks with permanent and thermoreversible cross-links. *Soft Matter*, 2010, **6**, 3548–3561.

99. J.F. Douglas, Influence of Chain Structure and Swelling on the Elasticity of Rubbery Materials: Localization Model Description. *Macromol. Symp.* 2013, **329**, 87–100.

100. L.J. Gibson, M.F. Ashby and B.A. Harley, Cellular materials in nature and medicine. 2010, Cambridge, UK: Cambridge University Press.

101. I. Levental, P.C. Georges and P.A. Janmey, Soft biological materials and their impact on cell function. Soft Matter, 2007, **3**, 299 – 306.

102. L.A. Mihai, L. Chin, P.A. Janmey and A. Goriely, A comparison of hyperelastic constitutive models applicable to brain and fat tissues. *J. R. Soc. Interface*, 2015, **12**, 20150486.

103. B.D. Ermi and E.J. Amis, Influence of backbone solvation on small angle neutron scattering from polyelectrolyte solutions. *Macromolecules* 1997, **30**, 6937–6942.

104. D. Wang, J. Lal. D. Moses, G.C. Bazan and A. Heeger, Small angle neutron scattering (SANS) studies of a conjugated polyelectrolyte in aqueous solution. *J. Chem. Phys. Lett.* 2001, **348**, 411–415.

105. T.Suzuki, T. Karino, F. Ikkai and M. Shibayama, pH Dependence of Macroscopic Swelling and Microscopic Structures for Thermo/pH-Sensitive Gels with Different Charge Distribution, Macromolecules 2008, 41, 9882-9889.

106. F. Horkay and P.J. Basser, Composite Hydrogel Model of Cartilage Predicts Its Load Bearing Ability. *Scientific Reports,* 2020, **10**, 8103.

107. J.F. Mansour and J.M. Welter, Multimodal evaluation of tissue-engineered cartilage. *J Med Biol Eng.* 2013, **33**, 1–16.

108. A.K. Pappa, M. Caballero, R.G. Dennis, M.D. Skancke, R.J. Narayan, J.P. Dahl and J.A. van Aalst, Biochemical Properties of Tissue-Engineered Cartilage, *J Craniofac Surg.* 2014, **25**, 111–115.

109. R.C.M. Revell and K.A. Athanasiou, Chondroitinase ABC Treatment Results in Greater Tensile Properties of Self-Assembled Tissue-Engineered Articular Cartilage. *Tissue Eng Part A.* 2009, **15**, 3119–3128.

110. S. Grenier, M.M. Bhargava and P.A. Torzilli, An *In Vitro* Model for the Pathological Degradation of Articular Cartilage in Osteoarthritis. *J Biomech.* 2014*, **47**, 645–652.